

# Cross-Modal Synergies: Unveiling the Potential of Motion-Aware Fusion Networks in Handling Dynamic and Static ReID Scenarios

Fuxi Ling  
Hangzhou Dianzi University  
lingfuxi@gmail.com

Guoqiang Huang  
Zhejiang Gongshang University  
guoqianghuang@mail.zjgsu.edu.cn

Hong Wu  
Hangzhou Dianzi University  
wuhong.wh@gmail.com

Hongye Liu  
China Jiliang University  
hongyeliu@mail.cjlu.edu.cn

Jing Li  
Zhejiang Gongshang University  
jingli@mail.zjgsu.edu.cn

Zhihao Tang  
Hangzhou Dianzi University

## Abstract

*Navigating the complexities of person re-identification (ReID) in varied surveillance scenarios, particularly when occlusions occur, poses significant challenges. We introduce an innovative Motion-Aware Fusion (MOTAR-FUSE) network that utilizes motion cues derived from static imagery to significantly enhance ReID capabilities. This network incorporates a dual-input visual adapter capable of processing both images and videos, thereby facilitating more effective feature extraction. A unique aspect of our approach is the integration of a motion consistency task, which empowers the motion-aware transformer to adeptly capture the dynamics of human motion. This technique substantially improves the recognition of features in scenarios where occlusions are prevalent, thereby advancing the ReID process. Our comprehensive evaluations across multiple ReID benchmarks, including holistic, occluded, and video-based scenarios, demonstrate that our MOTAR-FUSE network achieves superior performance compared to existing approaches.*

## 1. Introduction

In contemporary urban landscapes, the surge in population and infrastructural density necessitates sophisticated surveillance solutions that can effectively manage public safety and streamline security operations. Person re-identification (ReID) has become integral to these systems, enabling the identification of individuals across dispersed surveillance cameras with varying perspectives and con-

ditions [23, 49, 51, 52, 61]. The deployment of ReID spans multiple domains from enhancing public safety initiatives to optimizing retail customer experiences, marking its significance in both civil and commercial sectors [3, 10, 16, 47, 55, 56].

The evolution of ReID technology over recent years has been catalyzed by breakthroughs in deep learning, which have substantially refined the accuracy of identifying unobscured subjects. Nevertheless, the application of ReID in natural, uncontrolled settings is frequently hampered by challenges such as inconsistent lighting, physical blockages, and the limited field of view from stationary cameras [30, 46].

The static nature of traditional image-based ReID frameworks often falls short in dynamic urban environments where human activity is fluid and unpredictable. These systems struggle to capture the sequential and behavioral subtleties crucial for recognizing individuals in densely populated areas where visual obstructions are common [26, 37, 42].

In response to these limitations, there has been a pivot towards video-based ReID approaches. These methods exploit the rich temporal data inherent in video streams, offering enhanced capabilities in scenarios plagued by frequent occlusions or pronounced variations in individual poses [1, 9]. By analyzing sequences of movements, video-based systems provide a deeper insight into behavioral patterns, substantially aiding in the distinction of persons in crowded scenes.

Our novel Motion-Aware Fusion (MOTAR-FUSE) network is designed to synthesize the strengths of both static and dynamic analysis techniques. MOTAR-FUSE utilizes

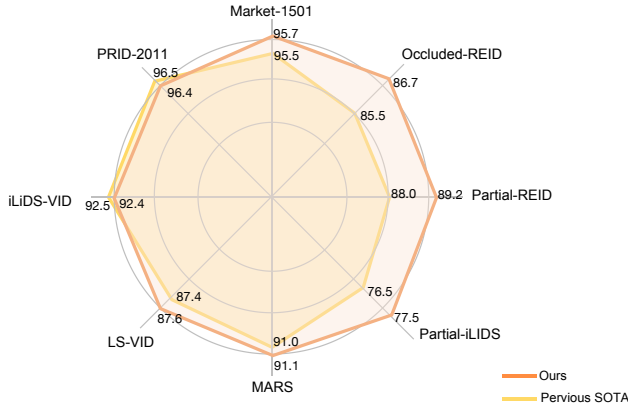


Figure 1. Graphical depiction of MOTAR-FUSE’s comparative advantage over standard ReID models in diverse operational contexts.

inferred motion from static images, a method traditionally employed in video processing, to augment the identification process in image-based systems. This synthesis allows for a comprehensive analysis that addresses the typical challenges of occlusions and environmental variability found in urban surveillance settings [4].

This transformative approach not only remedies the deficits of previous systems but also adapts seamlessly to the complexities of real-world surveillance. Extensive testing across varied ReID benchmarks underscores MOTAR-FUSE’s unparalleled efficacy, particularly in environments characterized by intricate occlusions and fluctuating conditions. Our findings affirm MOTAR-FUSE’s potential to redefine the operational capabilities of urban security systems.

## 2. Related Work

This section outlines key developments in the domain of person re-identification (ReID), underscoring major advancements in image-based identification and the innovative use of motion data through advanced segmentation techniques, which have significantly shaped our research approach.

### 2.1. Image Person Re-Identification

Image-based person ReID, covering both holistic and partial visibility scenarios, focuses on the consistent identification of individuals from different camera perspectives. The expansion of comprehensive datasets [15,29,38,39,43] combined with breakthroughs in deep learning, particularly through the use of transformer technologies, has considerably advanced our capability to extract nuanced human features. This advancement has set new standards in holistic ReID tasks. For example, TransReID [13,24] integrates a

transformer with unique modules like a jigsaw patch mechanism and side information embeddings, thereby enhancing performance significantly. Efforts have also been concentrated on overcoming challenges related to occlusion. For instance, PAT [22] utilizes a novel encoder-decoder structure with adaptable part prototypes dedicated to occluded ReID situations, achieving noteworthy outcomes. Moreover, FED [46] targets improvements against obstructions with strategic data augmentation and introduces mechanisms for erasing occlusions and diffusing features, enhancing the clarity of pedestrian identification. DPM [36] leverages a hierarchical mask generator to enhance the overall prototype and maintain a comprehensive imagery dataset, facilitating seamless alignment without external aids. Despite progress, the efficacy of these models is often limited by unexpected occlusions and predominantly relies on visual cues from subjects [27,33,43,54].

### 2.2. Video Person Re-Identification

Video-based ReID utilizes temporal data to address common issues like occlusion and motion blur found in static-image methods. This modality gains from immediate access to motion analytics and optical flow, thereby improving identification precision. Prominent methods involve temporal attention mechanisms that highlight important frames and disregard those of lower quality, and the use of self-attention or Graph Convolutional Networks (GCNs) [7,8,40,41] to bolster temporal linkages and dependencies among frames. A particular methodology [6,50] merges an RNN-mask framework with a pre-trained keypoint detector to derive elaborate motion and local part features. Another distinct strategy, the mutual attention network [18], applies optical flow in a Siamese network setting to extract essential spatiotemporal features for ReID. SBM [3] introduces a temporal relation-based method that enhances differential analyses for richer representations, although such approaches often face challenges with the integration of global-range features and are computationally intensive.

### 2.3. Motion-Guided Segmentation

In the area of motion-guided segmentation, Siarohin *et al.* [32] have innovated a self-supervised learning strategy that leverages motion details for effective segmentation of human parts. This methodology, drawing from foundational efforts [17,31,58], uses a reconstruction objective to dissect semantic and appearance attributes separately. While this is resource-intensive, it furnishes critical insights into how motion data can distinguish human elements and provide latent motion indicators, profoundly influencing our approach.

Distinctly, our methodology efficiently handles both image- and video-based ReID tasks with a novel motion-aware transformer that directly extracts motion data from

static images, enhancing the feature set for ReID. This dual capability underscores our method’s innovation, distinguishing it from conventional strategies in the field.

### 3. Methodology

Our Motion-Aware ReID system is engineered to exploit spatial and temporal data derived from static images, thereby significantly enhancing the accuracy of person re-identification. The system architecture, illustrated on the left side of Fig. 2, integrates several key components: a **visual encoder**, a **visual adapter**, a **motion-aware module**, and a **fusion encoder**.

The visual encoder initiates the process by capturing detailed spatial features from the entire image. These features are subsequently converted into a series of visual tokens by the visual adapter. The motion-aware module processes these tokens to extract dynamic motion tokens, which, along with a hybrid class token, feed into the fusion encoder producing the final output used in pedestrian identification.

#### 3.1. Visual Encoder & Visual Adapter

Refer to Fig. 2 (b) for a diagram of this component. Utilizing a pre-trained Vision Transformer (ViT-B/16) [4], the visual encoder outperforms conventional convolutional networks by analyzing complex image backgrounds more effectively. Training involves pairing images within each batch to compute motion consistency loss, which is detailed in Section 3.2. The images are dissected into patches, linearly projected to a uniform vector size across all layers, and enhanced with positional embeddings to enrich the visual features.

The visual adapter then condenses these enhanced features into visual tokens, optimizing computational efficiency while retaining essential spatio-temporal information. This module’s adaptability to various media inputs is achieved by adjusting the frame count and modifying positional embeddings to suit different input types.

#### 3.2. Motion-Aware Transformer

Illustrated in Fig. 2-(c), this module transforms visual tokens into motion tokens through a sequence of operations. A cross-attention layer initially isolates specific human body parts from the visual tokens, which are then refined into motion tokens by subsequent self-attention and feed-forward layers, capturing essential dynamic information. We introduce a specialized motion consistency task with a custom loss function to ensure the transformer’s efficacy during training, particularly effective when processing single-image inputs at inference.

#### 3.3. Fusion Encoder

This encoder amalgamates visual and motion tokens into a unified representation, encapsulated in a hybrid class token. This comprehensive token, processed through an advanced transformer-based encoder, captures an integrated representation of human features crucial for effective ReID. The encoder outputs an additional token vital for the final identification tasks, integrating linear projections of both token types and enabling their integration through sophisticated cross-attention mechanisms.

#### 3.4. Training and Inference

End-to-end training of the system begins with a stabilization phase using video datasets to solidify motion token generation. The model is refined using a hybrid loss function that combines cross-entropy and triplet loss, optimizing the system for precise pedestrian identification.

During inference, the output from the fusion encoder, particularly the hybrid class token, serves as the primary feature set for retrieval tasks, ensuring accurate and efficient person re-identification across diverse scenarios. This method maximizes the utilization of spatial and temporal data inherent in human movements, as expressed by the following equations:

$$\mathcal{L} = \lambda_g \mathcal{L}_g + \lambda_{mc} \mathcal{L}_{mc}, \tag{1}$$

where  $\lambda_g$  and  $\lambda_{mc}$  are scaling factors for the cross-entropy loss  $\mathcal{L}_g$  and motion consistency loss  $\mathcal{L}_{mc}$  respectively:

$$\mathcal{L}_g = \mathcal{L}_c(h_{m.cls}) + \mathcal{L}_t(h_{m.cls}), \tag{2}$$

where  $h_{m.cls}$  are the outputs of the fusion encoder,  $\mathcal{L}_c$  represents the cross-entropy loss, and  $\mathcal{L}_t$  represents the triplet loss.

### 4. Experiments

This section delineates the empirical validation of our Motion-Aware ReID framework. We outline the setup, engage in a comprehensive evaluation using several benchmark datasets for image and video ReID, and conclude with detailed ablation studies to assess the impact of specific system components.

#### 4.1. Datasets and Evaluation Metrics

Our evaluation leverages a variety of datasets designed to challenge and verify the robustness of ReID systems under diverse conditions: - **Market-1501** [59] is employed to assess our model’s performance in environments with minimal occlusions. - For scenarios with partial visibility, we utilize **Partial-iLIDS** [60] and **Partial REID** [62], which include images with manually occluded regions. -

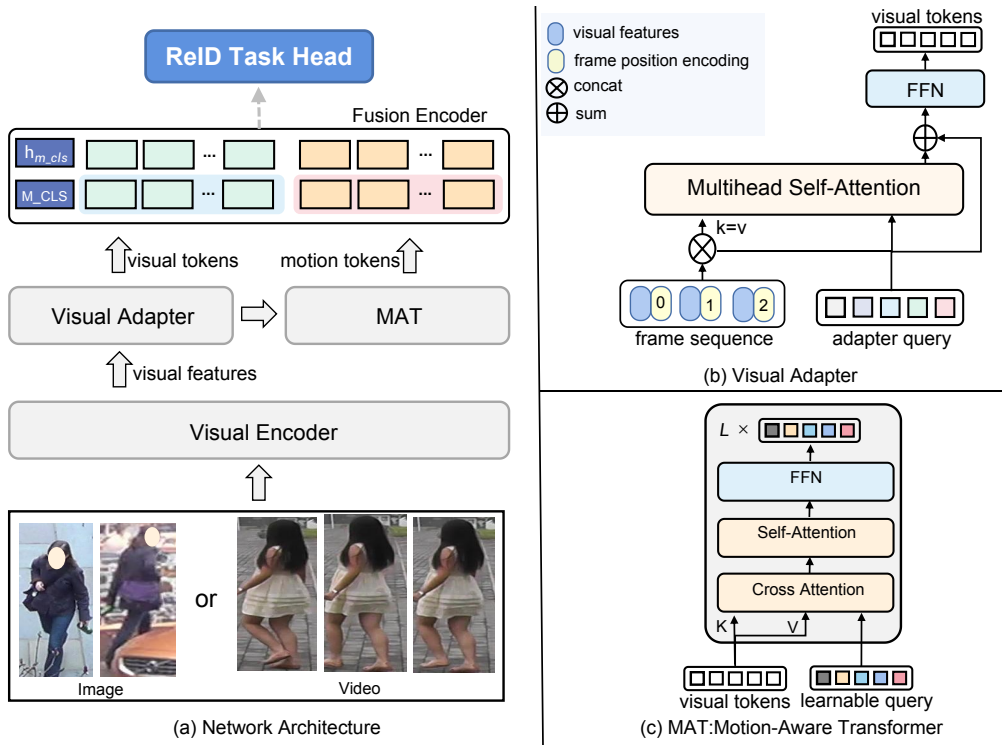


Figure 2. An overview of the proposed MOTAR-FUSE module.

Table 1. Performance comparison with state-of-the-arts on MARS, LS-VID, iLiDS-VID, and PRID-2011 datasets. Our method achieves competitive performance on four datasets.

| Method       | MARS        |             | LS-VID      |             | iLiDS-VID   |             | PRID-2011   |              |
|--------------|-------------|-------------|-------------|-------------|-------------|-------------|-------------|--------------|
|              | Rank-1      | mAP         | Rank-1      | mAP         | Rank-1      | Rank-5      | Rank-1      | Rank-5       |
| M3D [21]     | 84.4        | 74.1        | 57.7        | 40.1        | 74.0        | 94.3        | 94.4        | <b>100.0</b> |
| AP3D [10]    | 90.1        | 85.1        | 84.5        | 73.2        | 88.7        | -           | -           | -            |
| GRL [25]     | 91.0        | 84.8        | -           | -           | 90.4        | 98.3        | 96.2        | 99.7         |
| GLTR [19]    | 87.0        | 78.5        | 63.1        | 44.3        | 86.0        | 98.0        | 95.5        | <b>100.0</b> |
| MGH [48]     | 90.0        | 85.8        | -           | -           | 85.6        | 97.1        | 94.8        | 99.3         |
| MG-RAFA [53] | 88.8        | 85.9        | -           | -           | 88.6        | 98.0        | 95.9        | 99.7         |
| STMN [5]     | 90.5        | 84.5        | 82.1        | 69.2        | 91.5        | -           | -           | -            |
| CAViT [47]   | 90.8        | 87.2        | 89.2        | 79.2        | 93.3        | <b>98.0</b> | 95.5        | 98.9         |
| SINet [2]    | 91.0        | 86.2        | 87.4        | 79.6        | <b>92.5</b> | -           | <b>96.5</b> | -            |
| <b>Ours</b>  | <b>91.1</b> | <b>86.4</b> | <b>87.6</b> | <b>79.9</b> | 92.4        | 97.9        | 96.4        | <b>100.0</b> |

**Occluded REID** [64] tests our model’s efficacy in handling severe occlusions. - Video-based datasets such as **MARS** [57], **LS-VID** [20], **iLiDS-VID** [45], and **PRID-2011** [14] provide dynamic sequences that are crucial for evaluating temporal attribute handling.

Performance metrics include Cumulative Matching Characteristic (CMC) curves and mean average precision (mAP), which offer insights into the ranking accuracy and retrieval quality of our model.

## 4.2. Implementation Details

For consistency, all processed images and video frames are resized to  $256 \times 128$ . The network utilizes  $16 \times 16$  patches. Training parameters include a batch size of 32 clips per batch for video data, accommodating 8 identities, and similar configurations for image data. The system is optimized over 120 epochs using the Adam optimizer, with an added emphasis on data augmentation techniques such as random flipping and erasing to enhance model robustness.

### 4.3. Comparative Analysis

Our method is compared with several state-of-the-art approaches across different datasets, indicating its competitive edge, particularly in handling complex scenarios like occlusions and dynamically captured sequences.

#### Performance on Video-based and Holistic Datasets:

Our evaluations on datasets like MARS and LS-VID demonstrate superior performance, particularly in terms of Rank-1 accuracy and mAP, underscoring the effectiveness of the visual adapter in distilling spatio-temporal features.

Table 2. Comparison of performance metrics on Market-1501 with state-of-the-art methods.

| Method         | Rank-1      | mAP         |
|----------------|-------------|-------------|
| FPR [12]       | 95.4        | 86.6        |
| PCB [35]       | 92.3        | 77.4        |
| PGFA [28]      | 91.2        | 76.8        |
| VPM [34]       | 93.0        | 80.8        |
| HOReID [44]    | 94.2        | 84.9        |
| ISP [63]       | 95.3        | 88.6        |
| PAT [22]       | 95.4        | 88.0        |
| TransReID [13] | 95.0        | 88.2        |
| FED [46]       | 95.0        | 86.3        |
| DPM [36]       | 95.5        | 89.7        |
| <b>Ours</b>    | <b>95.7</b> | <b>89.8</b> |

### 4.4. Ablation Studies

To dissect the contributions of specific components, we perform several ablation studies: - **Effect of the Motion Consistency Task:** Removing this component significantly diminishes performance on occluded datasets, reinforcing its necessity for handling complex occlusions effectively. - **Impact of Pre-training on Video Datasets:** Pre-training enhances the motion-aware transformer’s effectiveness, providing it with vital motion insights essential for robust performance across static and dynamic scenes.

These experiments underline the strengths and adaptive capabilities of our ReID system, particularly its proficiency in handling real-world challenges posed by occlusions and dynamic environments.

### 4.5. Detailed Analysis of Learnable Query Length in Motion-Aware Transformer

The configuration of learnable queries within the motion-aware transformer is crucial as it directly influences the model’s ability to dissect and analyze the human body into distinct parts. Our experiments investigate the impact of varying the query length on the model’s performance across several ReID benchmarks, providing insights into the optimal structuring of these queries.

Table 3. Performance comparison with other methods on occluded-REID dataset.

| Method         | Occluded-REID |             |
|----------------|---------------|-------------|
|                | Rank-1        | mAP         |
| FPR [12]       | 78.3          | 68.0        |
| PCB [35]       | 41.3          | 38.9        |
| AMC+SWM [62]   | 31.2          | 27.3        |
| PVPM [8]       | 70.4          | 61.2        |
| HOReID [44]    | 80.3          | 70.2        |
| PAT [22]       | 81.6          | 72.1        |
| TransReID [13] | 70.2          | 67.3        |
| DPM [36]       | 85.5          | 79.7        |
| <b>Ours</b>    | <b>86.7</b>   | <b>81.2</b> |

Table 4. Performance comparison with other methods on Partial REID dataset, and Partial-iLIDS dataset.

| Method       | Partial-REID |             | Partial-iLIDS |             |
|--------------|--------------|-------------|---------------|-------------|
|              | Rank-1       | Rank-3      | Rank-1        | Rank-3      |
| SFR [11]     | 56.9         | 78.5        | 63.9          | 74.8        |
| FPR [12]     | 81.0         | -           | 68.1          | -           |
| AMC+SWM [62] | 37.3         | 46.0        | 21.0          | 32.8        |
| PVPM [8]     | 78.3         | 87.7        | -             | -           |
| PGFA [28]    | 68.0         | 80.0        | 69.1          | 80.9        |
| VPM [34]     | 67.7         | 81.9        | 65.5          | 74.8        |
| HOReID [44]  | 85.3         | 91.0        | 72.6          | 86.4        |
| PAT [22]     | 88.0         | 92.3        | 76.5          | 88.2        |
| FED [46]     | 84.6         | -           | -             | -           |
| <b>Ours</b>  | <b>89.2</b>  | <b>93.2</b> | <b>77.5</b>   | <b>89.6</b> |

Table 5. The experiments of motion consistency task on Market-1501, Occluded-REID, Partial-REID and MARS. Here, O-REID is the abbreviation of Occluded-REID and P-REID is the abbreviation of Partial-REID.

| Method | Market-1501 | O-REID      | P-REID      | MARS        |
|--------|-------------|-------------|-------------|-------------|
|        | Rank-1      | Rank-1      | Rank-1      | Rank-1      |
| w      | <b>95.7</b> | <b>86.7</b> | <b>89.2</b> | <b>91.1</b> |
| w/o    | 94.9        | 83.9        | 83.6        | 90.5        |

#### 4.5.1 Experimental Setup and Findings

We systematically varied the length of the learnable queries in the transformer and assessed the model’s performance on datasets like Market-1501, Occluded-REID, Partial-REID, and MARS. The purpose was to determine how the granularity of body part segmentation affects overall identification accuracy.

#### Results Discussion:

- The optimal performance, as evidenced by the highest Rank-1 accuracy, was consistently observed at a query length of 10. This suggests a balanced level of detail that aids effective person re-identification without

Table 6. The experiments on the length of learnable queries in MOTAR-FUSE on different benchmarks.

| Length | Market-1501<br>Rank-1 | O-REID<br>Rank-1 | P-REID<br>Rank-1 | MARS<br>Rank-1 |
|--------|-----------------------|------------------|------------------|----------------|
| 2      | 94.0                  | 84.0             | 83.7             | 89.9           |
| 4      | 94.4                  | 84.3             | 84.2             | 90.1           |
| 6      | 95.0                  | 85.7             | 86.3             | 90.4           |
| 8      | 95.2                  | 86.3             | 88.9             | 90.9           |
| 10     | <b>95.7</b>           | <b>86.7</b>      | <b>89.2</b>      | <b>91.1</b>    |
| 16     | 95.4                  | 85.2             | 88.1             | 90.9           |
| 32     | 95.0                  | 84.1             | 84.0             | 90.5           |

Table 7. The experiments on whether pre-trained on video dataset. Here, O-REID is the abbreviation of Occluded-REID and P-REID is the abbreviation of Partial-REID.

| Method | O-REID      |             | P-REID      |             |
|--------|-------------|-------------|-------------|-------------|
|        | Rank-1      | mAP         | Rank-1      | Rank-3      |
| w      | <b>86.7</b> | <b>81.2</b> | <b>89.2</b> | <b>93.2</b> |
| w/o    | 86.1 (-0.6) | 79.8(-0.4)  | 88.5(-0.7)  | 92.7(-0.5)  |

overwhelming the model with excessive granularity.

- When the query length exceeded 10, a notable decrease in performance was observed, particularly on datasets characterized by occlusion and partial visibility (see Tab. 6). This decline indicates the potential pitfalls of over-segmentation, where the model may become prone to errors due to an overly fragmented representation of the human figure.
- In contrast, the impact on datasets focused on holistic ReID tasks was less pronounced, underscoring the reliance on global features under less challenging conditions.

These observations underscore the dual functionality of the fusion encoder, which adeptly integrates both local and global features, enhancing the robustness of the resulting feature representation  $h_{m.cls}$ .

#### 4.5.2 Comparative Analysis with Previous Methods

In reviewing earlier human part-based approaches, a common limitation is their reliance on part-aware masks that may inadvertently emphasize background elements, due to high confidence allocations to non-crucial areas. Such designs, while effective under certain conditions, exhibit vulnerabilities in complex occluded environments.

**Our Approach:** By integrating motion information derived from static images through a sophisticated motion

consistency task, our model extends beyond mere appearance features to incorporate dynamic aspects. This integration significantly enhances the model’s resilience and adaptability, enabling robust performance even in scenarios rife with occlusions.

These experiments validate the superiority of a balanced approach to part segmentation within our motion-aware transformer, particularly emphasizing the importance of motion information in enhancing the discriminative power of the learned features, crucial for tackling complex real-world ReID challenges.

#### 4.6. Influence of Pre-training on Video Datasets

One pivotal aspect of our methodology involves the utilization of pre-training on video datasets to enhance the motion-aware transformer’s ability to process static images. This section evaluates the impact of this pre-training on the overall performance of our ReID system.

##### 4.6.1 Effect of Video Pre-training

Pre-training the motion-aware transformer on video data is intended to endow the model with preliminary motion insights, which are crucial for handling static images effectively. As demonstrated in Table 7, omitting this pre-training phase results in a slight but noticeable decrease in performance, specifically a reduction of approximately 0.6 to 0.7% in Rank-1 accuracy and about 0.5% in mean Average Precision (mAP). This shows the significant role of motion-derived knowledge in enhancing the predictive prowess of our model.

Although the visual adapter significantly aids in acquiring motion knowledge from video data, it’s crucial to note that our system is robust enough to be trained from scratch if necessary. However, in the absence of video pre-training, the model requires more epochs to reach a comparable level of performance, highlighting the efficiency gains provided by this preliminary step.

##### 4.6.2 Visualization and Analysis of Human Part Segmentation

To further illustrate the practical benefits of integrating motion information, we provide visualizations of human part segmentation achieved through the motion consistency task.

Figure 3 reveals how the addition of motion information refines the attention mechanism of our model: - **Fig. 3-(a)** presents an attention map where the model, informed by motion cues, concentrates more effectively on the human body, even in complex environments. This enhancement is crucial for improving resistance to occlusions and background noise. - **Fig. 3-(b)** depicts a scenario where a pedestrian is occluded by a bicycle. Despite the occlusion, our model effectively discriminates between the hu-

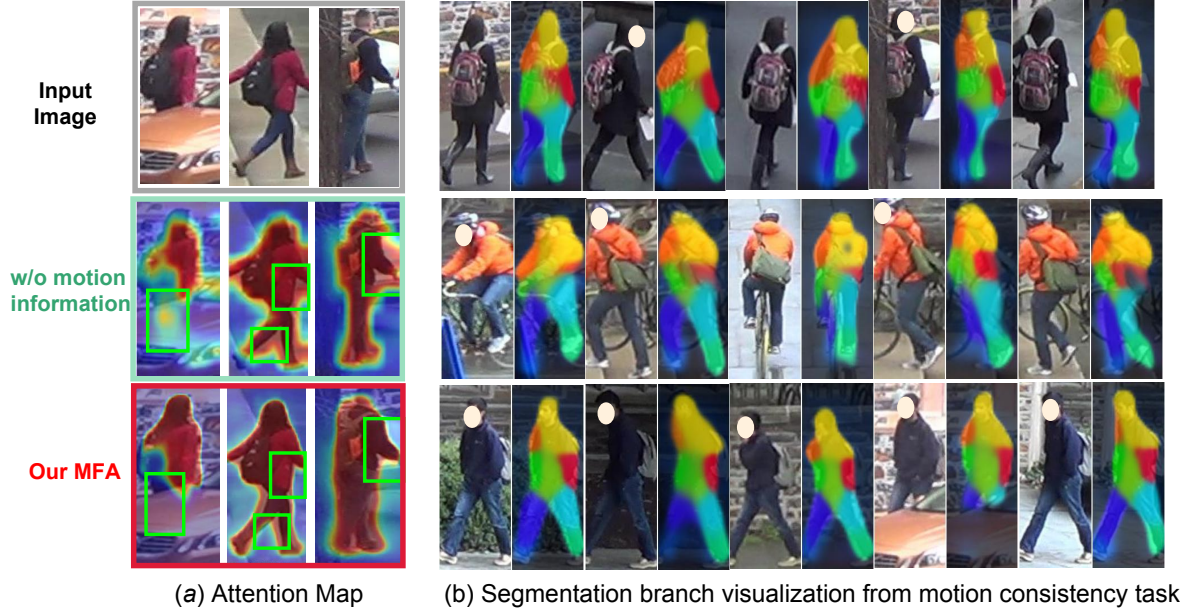


Figure 3. Visualization of human part segmentation under different conditions: (a) shows enhanced focus on the human body in a cluttered scene; (b) demonstrates robust segmentation when the subject is partially occluded by a bike.

man and non-human elements, maintaining accurate segmentation and identification.

These visualizations underscore the effectiveness of motion information in refining the model’s ability to handle real-world variability in human appearances, particularly in occluded scenarios. By learning to focus on dynamic human parts, the system demonstrates superior adaptability and accuracy, proving the value of motion data in static image ReID tasks.

## 5. Conclusion and Future Work

This study has significantly advanced the integration of motion information in person re-identification by developing an innovative motion-aware fusion network. Our system stands out by proficiently processing both image and video data, facilitated by a versatile visual adapter. This dual capability enhances the applicability of our model across a variety of real-world scenarios, bridging the gap between static image analysis and dynamic video processing.

Our approach extends the extraction of motion information to still images, a notable enhancement over traditional methods that rely solely on video data. By enabling the fusion encoder to intricately merge visual features with derived motion data, we provide a richer, more nuanced representation of subjects. This enhanced feature integration has led to the establishment of new benchmarks on several ReID datasets, showcasing superior results in both holistic views and occluded scenarios, alongside robust perfor-

mance in video-based evaluations.

### 5.1. Achievements

The successful implementation of our model has demonstrated its efficacy in various testing environments, achieving state-of-the-art results on well-regarded benchmarks such as Market-1501, Occluded REID, and MARS. These achievements underscore the effectiveness of our method in addressing some of the most challenging aspects of person re-identification, including handling occlusions and extracting useful information from static images.

### 5.2. Limitations and Future Directions

Despite these successes, our approach does have limitations, notably the reliance on extensive pre-training for the motion-aware transformer. This requirement can introduce additional computational overhead and extend the training duration, potentially impacting the scalability and efficiency of deployment in operational settings.

Future research will aim to refine the extraction and integration of spatio-temporal information, to reduce or eliminate the dependence on pre-training phases. Innovations could include the development of more sophisticated motion detection algorithms that require less historical data to train effectively or the implementation of novel neural network architectures that are inherently more adept at recognizing and interpreting motion patterns.

Additionally, we plan to explore the application of our methodology to emerging areas within ReID, such as cross-

domain adaptation and low-resource environments, where the ability to generalize from limited or varying data is crucial.

### **5.3. Continued Impact**

As we continue our research, we are committed to pushing the boundaries of person re-identification technology. By addressing the current limitations and exploring new applications, we aim to further enhance the robustness, accuracy, and practicality of ReID systems. Our ongoing efforts will focus on making these advanced technologies more accessible and effective in diverse and challenging environments.

In conclusion, this study not only sets a new standard in the field of person re-identification through the innovative use of motion data but also paves the way for future advancements that could revolutionize how these systems are developed and deployed in real-world scenarios.

## References

- [1] Anurag Arnab, Mostafa Dehghani, Georg Heigold, Chen Sun, Mario Lučić, and Cordelia Schmid. Vivit: A video vision transformer. In *ICCV*, 2021. 1
- [2] Shutao Bai, Bingpeng Ma, Hong Chang, Rui Huang, and Xilin Chen. Salient-to-broad transition for video person re-identification. In *CVPR*. 4
- [3] Shutao Bai, Bingpeng Ma, Hong Chang, Rui Huang, and Xilin Chen. Salient-to-broad transition for video person re-identification. In *CVPR*, 2022. 1, 2
- [4] Alexey Dosovitskiy, Lucas Beyer, Alexander Kolesnikov, Dirk Weissenborn, Xiaohua Zhai, Thomas Unterthiner, Mostafa Dehghani, Matthias Minderer, Georg Heigold, Sylvain Gelly, et al. An image is worth 16x16 words: Transformers for image recognition at scale. *arXiv preprint arXiv:2010.11929*, 2020. 2, 3
- [5] Chanho Eom, Geon Lee, Junghyup Lee, and Bumsub Ham. Video-based person re-identification with spatial and temporal memory networks. In *ICCV*, 2021. 4
- [6] Hao Feng, Qi Liu, Hao Liu, Jingqun Tang, Wengang Zhou, Houqiang Li, and Can Huang. Docpedia: Unleashing the power of large multimodal model in the frequency domain for versatile document understanding. *Science China Information Sciences*, 67(12):1–14, 2024. 2
- [7] Hao Feng, Zijian Wang, Jingqun Tang, Jinghui Lu, Wengang Zhou, Houqiang Li, and Can Huang. Unidoc: A universal large multimodal model for simultaneous text detection, recognition, spotting and understanding. *arXiv preprint arXiv:2308.11592*, 2023. 2
- [8] Shang Gao, Jingya Wang, Huchuan Lu, and Zimo Liu. Pose-guided visible part matching for occluded person reid. In *CVPR*, 2020. 2, 5
- [9] Yixiao Ge, Zhuowan Li, Haiyu Zhao, Guojun Yin, Shuai Yi, Xiaogang Wang, and Hongsheng Li. Fd-gan: Pose-guided feature distilling gan for robust person re-identification. *arXiv preprint arXiv:1810.02936*, 2018. 1
- [10] Xinqian Gu, Hong Chang, Bingpeng Ma, Hongkai Zhang, and Xilin Chen. Appearance-preserving 3d convolution for video-based person re-identification. In *ECCV*, 2020. 1, 4
- [11] Lingxiao He, Zhenan Sun, Yuhao Zhu, and Yunbo Wang. Recognizing partial biometric patterns. *arXiv preprint arXiv:1810.07399*, 2018. 5
- [12] Lingxiao He, Yinggang Wang, Wu Liu, He Zhao, Zhenan Sun, and Jiashi Feng. Foreground-aware pyramid reconstruction for alignment-free occluded person re-identification. In *ICCV*, 2019. 5
- [13] Shuting He, Hao Luo, Pichao Wang, Fan Wang, Hao Li, and Wei Jiang. Transreid: Transformer-based object re-identification. In *CVPR*, 2021. 2, 5
- [14] Martin Hirzer, Csaba Beleznai, Peter M Roth, and Horst Bischof. Person re-identification by descriptive and discriminative classification. In *SCIA*, 2011. 4
- [15] Ruibing Hou, Hong Chang, Bingpeng Ma, Rui Huang, and Shiguang Shan. Bicnet-tks: Learning efficient spatial-temporal representation for video person re-identification. In *CVPR*, 2021. 2
- [16] Ruibing Hou, Bingpeng Ma, Hong Chang, Xinqian Gu, Shiguang Shan, and Xilin Chen. Interaction-and-aggregation network for person re-identification. In *CVPR*, pages 9317–9326, 2019. 1
- [17] Tomas Jakab, Ankush Gupta, Hakan Bilen, and Andrea Vedaldi. Unsupervised learning of object landmarks through conditional image generation. *NIPS*, 2018. 2
- [18] Madhu Kiran, Amran Bhuiyan, Louis-Antoine Blais-Morin, Ismail Ben Ayed, Eric Granger, et al. Flow guided mutual attention for person re-identification. *Image and Vision Computing*, 2021. 2
- [19] Jianing Li, Jingdong Wang, Qi Tian, Wen Gao, and Shiliang Zhang. Global-local temporal representations for video person re-identification. In *ICCV*, 2019. 4
- [20] Jianing Li, Jingdong Wang, Qi Tian, Wen Gao, and Shiliang Zhang. Global-local temporal representations for video person re-identification. In *CVPR*, 2019. 4
- [21] Jianing Li, Shiliang Zhang, and Tiejun Huang. Multi-scale 3d convolution network for video based person re-identification. In *AAAI*, 2019. 4
- [22] Yulin Li, Jianfeng He, Tianzhu Zhang, Xiang Liu, Yongdong Zhang, and Feng Wu. Diverse part discovery: Occluded person re-identification with part-aware transformer. In *CVPR*, 2021. 2, 5
- [23] Shengcai Liao, Yang Hu, Xiangyu Zhu, and Stan Z Li. Person re-identification by local maximal occurrence representation and metric learning. In *CVPR*, 2015. 1
- [24] Hongye Liu and Xiai Chen. Rethink motion information for occluded person re-identification. *Applied Sciences*, 14(6):2558, 2024. 2
- [25] Xuehu Liu, Pingping Zhang, Chenyang Yu, Huchuan Lu, and Xiaoyun Yang. Watching you: Global-guided reciprocal learning for video-based person re-identification. In *CVPR*, 2021. 4
- [26] Yuliang Liu, Jiaxin Zhang, Dezhi Peng, Mingxin Huang, Xinyu Wang, Jingqun Tang, Can Huang, Dahua Lin, Chunhua Shen, Xiang Bai, et al. Spts v2: single-point scene text spotting. *IEEE Transactions on Pattern Analysis and Machine Intelligence*, 2023. 1
- [27] Jinghui Lu, Haiyang Yu, Yanjie Wang, Yongjie Ye, Jingqun Tang, Ziwei Yang, Binghong Wu, Qi Liu, Hao Feng, Han Wang, et al. A bounding box is worth one token: Interleaving layout and text in a large language model for document understanding. *arXiv preprint arXiv:2407.01976*, 2024. 2
- [28] Jiaxu Miao, Yu Wu, Ping Liu, Yuhang Ding, and Yi Yang. Pose-guided feature alignment for occluded person re-identification. In *ICCV*, 2019. 5
- [29] Bin Shan, Xiang Fei, Wei Shi, An-Lan Wang, Guozhi Tang, Lei Liao, Jingqun Tang, Xiang Bai, and Can Huang. Mct-bench: Multimodal cognition towards text-rich visual scenes benchmark. *arXiv preprint arXiv:2410.11538*, 2024. 2
- [30] Charu Sharma, Siddhant R Kapil, and David Chapman. Person re-identification with a locally aware transformer. *arXiv preprint arXiv:2106.03720*, 2021. 1
- [31] Aliaksandr Siarohin, Stéphane Lathuilière, Sergey Tulyakov, Elisa Ricci, and Nicu Sebe. First order motion model for image animation. *NIPS*, 2019. 2

- [32] Aliaksandr Siarohin, Subhankar Roy, Stéphane Lathuilière, Sergey Tulyakov, Elisa Ricci, and Nicu Sebe. Motion-supervised co-part segmentation. In *ICPR*, 2021. 2
- [33] Wenhao Sun, Benlei Cui, Jingqun Tang, and Xue-Mei Dong. Attentive eraser: Unleashing diffusion model’s object removal potential via self-attention redirection guidance. *arXiv preprint arXiv:2412.12974*, 2024. 2
- [34] Yifan Sun, Qin Xu, Yali Li, Chi Zhang, Yikang Li, Shengjin Wang, and Jian Sun. Perceive where to focus: Learning visibility-aware part-level features for partial person re-identification. In *CVPR*, 2019. 5
- [35] Yifan Sun, Liang Zheng, Yi Yang, Qi Tian, and Shengjin Wang. Beyond part models: Person retrieval with refined part pooling (and a strong convolutional baseline). In *ECCV*, 2018. 5
- [36] Lei Tan, Pingyang Dai, Rongrong Ji, and Yongjian Wu. Dynamic prototype mask for occluded person re-identification. In *ACM MM*, 2022. 2, 5
- [37] Jingqun Tang, Weidong Du, Bin Wang, Wenyang Zhou, Shuqi Mei, Tao Xue, Xing Xu, and Hai Zhang. Character recognition competition for street view shop signs. *National Science Review*, 10(6):nwad141, 2023. 1
- [38] Jingqun Tang, Chunhui Lin, Zhen Zhao, Shu Wei, Binghong Wu, Qi Liu, Hao Feng, Yang Li, Siqi Wang, Lei Liao, et al. Textsquare: Scaling up text-centric visual instruction tuning. *arXiv preprint arXiv:2404.12803*, 2024. 2
- [39] Jingqun Tang, Qi Liu, Yongjie Ye, Jinghui Lu, Shu Wei, Chunhui Lin, Wanqing Li, Mohamad Fitri Faiz Bin Mahmood, Hao Feng, Zhen Zhao, et al. Mtvqa: Benchmarking multilingual text-centric visual question answering. *arXiv preprint arXiv:2405.11985*, 2024. 2
- [40] Jingqun Tang, Wenming Qian, Luchuan Song, Xiena Dong, Lan Li, and Xiang Bai. Optimal boxes: boosting end-to-end scene text recognition by adjusting annotated bounding boxes via reinforcement learning. In *European Conference on Computer Vision*, pages 233–248. Springer, 2022. 2
- [41] Jingqun Tang, Su Qiao, Benlei Cui, Yuhang Ma, Sheng Zhang, and Dimitrios Kanoulas. You can even annotate text with voice: Transcription-only-supervised text spotting. In *Proceedings of the 30th ACM International Conference on Multimedia*, MM ’22, page 4154–4163, New York, NY, USA, 2022. Association for Computing Machinery. 2
- [42] Jingqun Tang, Wenqing Zhang, Hongye Liu, MingKun Yang, Bo Jiang, Guanglong Hu, and Xiang Bai. Few could be better than all: Feature sampling and grouping for scene text detection. In *Proceedings of the IEEE/CVF Conference on Computer Vision and Pattern Recognition*, pages 4563–4572, 2022. 1
- [43] An-Lan Wang, Bin Shan, Wei Shi, Kun-Yu Lin, Xiang Fei, Guozhi Tang, Lei Liao, Jingqun Tang, Can Huang, and Wei-Shi Zheng. Pargo: Bridging vision-language with partial and global views. *arXiv preprint arXiv:2408.12928*, 2024. 2
- [44] Guan’an Wang, Shuo Yang, Huanyu Liu, Zhicheng Wang, Yang Yang, Shuliang Wang, Gang Yu, Erjin Zhou, and Jian Sun. High-order information matters: Learning relation and topology for occluded person re-identification. In *CVPR*, 2020. 5
- [45] Taiqing Wang, Shaogang Gong, Xiatian Zhu, and Shengjin Wang. Person re-identification by video ranking. In *ECCV*, 2014. 4
- [46] Zhikang Wang, Feng Zhu, Shixiang Tang, Rui Zhao, Lihuo He, and Jiangning Song. Feature erasing and diffusion network for occluded person re-identification. In *CVPR*, 2022. 1, 2, 5
- [47] Jinlin Wu, Lingxiao He, Wu Liu, Yang Yang, Zhen Lei, Tao Mei, and Stan Z Li. Cavit: Contextual alignment vision transformer for video object re-identification. In *ECCV*, 2022. 1, 4
- [48] Yichao Yan, Jie Qin, Jiaxin Chen, Li Liu, Fan Zhu, Ying Tai, and Ling Shao. Learning multi-granular hypergraphs for video-based person re-identification. In *CVPR*, 2020. 4
- [49] Yang Yang, Jimei Yang, Junjie Yan, Shengcai Liao, Dong Yi, and Stan Z Li. Salient color names for person re-identification. In *ECCV*, 2014. 1
- [50] Jiahang Yin, Ancong Wu, and Wei-Shi Zheng. Fine-grained person re-identification. *IJCV*, 2020. 2
- [51] Tianzhu Zhang, Changsheng Xu, and Ming-Hsuan Yang. Learning multi-task correlation particle filters for visual tracking. *PAMI*, 2018. 1
- [52] Tianzhu Zhang, Changsheng Xu, and Ming-Hsuan Yang. Robust structural sparse tracking. *PAMI*, 2018. 1
- [53] Zhizheng Zhang, Cuiling Lan, Wenjun Zeng, and Zhibo Chen. Multi-granularity reference-aided attentive feature aggregation for video-based person re-identification. In *CVPR*, 2020. 4
- [54] Weichao Zhao, Hao Feng, Qi Liu, Jingqun Tang, Shu Wei, Binghong Wu, Lei Liao, Yongjie Ye, Hao Liu, Wengang Zhou, et al. Tabpedia: Towards comprehensive visual table understanding with concept synergy. *arXiv preprint arXiv:2406.01326*, 2024. 2
- [55] Zhen Zhao, Jingqun Tang, Chunhui Lin, Binghong Wu, Can Huang, Hao Liu, Xin Tan, Zhizhong Zhang, and Yuan Xie. Multi-modal in-context learning makes an ego-evolving scene text recognizer. In *Proceedings of the IEEE/CVF Conference on Computer Vision and Pattern Recognition*, pages 15567–15576, 2024. 1
- [56] Zhen Zhao, Jingqun Tang, Binghong Wu, Chunhui Lin, Shu Wei, Hao Liu, Xin Tan, Zhizhong Zhang, Can Huang, and Yuan Xie. Harmonizing visual text comprehension and generation. *arXiv preprint arXiv:2407.16364*, 2024. 1
- [57] Liang Zheng, Zhi Bie, Yifan Sun, Jingdong Wang, Chi Su, Shengjin Wang, and Qi Tian. Mars: A video benchmark for large-scale person re-identification. In *ECCV*, 2016. 4
- [58] Liang Zheng, Yujia Huang, Huchuan Lu, and Yi Yang. Pose-invariant embedding for deep person re-identification. *TIP*, 2019. 2
- [59] Liang Zheng, Liyue Shen, Lu Tian, Shengjin Wang, Jingdong Wang, and Qi Tian. Scalable person re-identification: A benchmark. In *ICCV*, 2015. 3
- [60] Wei-Shi Zheng, Shaogang Gong, and Tao Xiang. Person re-identification by probabilistic relative distance comparison. In *CVPR*, 2011. 3
- [61] Wei-Shi Zheng, Shaogang Gong, and Tao Xiang. Reidentification by relative distance comparison. *PAMI*, 2012. 1

- [62] Wei-Shi Zheng, Xiang Li, Tao Xiang, Shengcai Liao, Jianhuang Lai, and Shaogang Gong. Partial person re-identification. In *ICCV*, 2015. 3, 5
- [63] Kuan Zhu, Haiyun Guo, Zhiwei Liu, Ming Tang, and Jinqiao Wang. Identity-guided human semantic parsing for person re-identification. In *ECCV*, 2020. 5
- [64] Jiaxuan Zhuo, Zeyu Chen, Jianhuang Lai, and Guangcong Wang. Occluded person re-identification. In *ICME*, 2018. 4